Sluggish response of untrapped electrons and global electrostatic micro-instabilities in a tokamak

2010 J. Phys.: Conf. Ser. 208 012058

(http://iopscience.iop.org/1742-6596/208/1/012058)

Journal of Physics: Conference Series **208** (2010) 012058 doi:10.1088/1742-6596/208/1/012058

Sluggish response of untrapped electrons and global electrostatic micro-instabilities in a tokamak

J. Chowdhury, R. Ganesh
Institute for Plasma Research, Bhat, Gandhinagar, India

P. Angelino
CEA/DSM/DRFC, Association Euratom-CEA, Cadarache,
13108 St Paul-lez-Durance, France

J. Vaclavik, L. Villard and S. Brunner
CRPP, Association EURATOM - Confédération Suisse,
EPFL, 1015 Lausanne, Switzerland

E-mail: jugal@ipr.res.in

Abstract. Electrons whether adiabatic or non-adiabatic play important role in determining the stability properties of a global electrostatic mode. In the present analysis, the effect of non-adiabaticity of electrons with all its kinetic effects is investigated for ion temperature gradient driven mode in the presence of fast ions using a linear gyro-kinetic code EM-GLOGYSTO-F.

1. Introduction

For the last few years extensive work has been going on both experimentally and theoretically to understand the cause of anomalous transport [1-3] in a tokamak that limits the confinement. The ion thermal transport[5] in the plasma is found to be due to temperature gradient driven modes (ITG) [4, 6]. ITG modes are reactive modes in the low frequency/low k regime. The earlier studies of ITG mode were restricted to adiabatic electrons (Boltzmann electrons) [7, 8]. The outcome of such an interpretation is that it makes the analysis more tractable and computation easier because no longer one needs to bother about the vastly separate response time-scales of electrons and ions because of their disparate masses. For the last few years attempts have been made to incorporate full electron dynamics into the physics of ion temperature gradient mode. Trapped electron coupled ITG has been studied extensively in [9-16]. Results showed that the addition of trapped electrons to adiabatic ITG is more than a mere modification and the growth rate was observed to increase by 2 to 3 times. The non-adiabaticity of electrons in these studies was brought about by the trapped fraction of electrons. However, the passing electrons also have a non-adiabatic part realized by various kinetic resonances and gradients. Effects of the passing electrons along with trapped electrons is studied in [17-19]. The motivation of the present work is the need of a model which invokes the full electron dynamics that is adiabaticity and non adiabaticity simultaneously for the passing fraction with no simplifying assumption. Energetic particles are another component in the fusion plasma that are indispensable and have significant

effect on the temperature gradient driven modes. These are produced in a hot plasma either by auxiliary heating schemes or in post fusion products as alpha particles. These fast ions carry a significant amount of β and therefore require a non-perturbative treatment rather than considering them a mere perturbation to the background plasma. We therefore consider fast ions on the same physics footing as that of background species namely ions and electrons. To meet these two requirements an existing gyrokinetic code EM-GLOGYSTO [20-26] is modified to take in to account the full electron dynamics and fast ions and renamed as EM-GLOGYSTO-F. It is a fully electro-magnetic and fully kinetic global gyrokinetic code. For the present work the set of model equations are reduced to zero beta limit to make it purely electrostatic. The equilibrium contains no electric field, collisions, Shafranov shift and geometry effect. Ions are considered to have a trapped fraction but electrons are not. Only passing fast ions are considered. The paper is organized as follow. Section *2* presents the model gyrokinetic equations. This is the basis for the development of the code EM-GLOGYSTO-F. Section *3.1* presents the results that compare the ITG mode without and with non-adiabatic passing electrons. Section *3.2* presents results showing the non-perturbative effect of fast ions on ITG mode. Finally section *4* produces a brief summary of the results.

2. Model equations

The perturbed density for species j (ion, electron and fast ions) in real space containing full dynamics can be obtained by using gyrokinetic theory

$$\tilde{n}_j(\mathbf{r};\omega) = -\left(\frac{q_j N}{T_j}\right)\left[\tilde{\varphi} + \int d\mathbf{k}\exp\left(\iota\mathbf{k}\cdot\mathbf{r}\right)\int d\mathbf{v}\frac{f_{Mj}}{N}\left(\omega-\omega_j^*\right)\left(\iota\mathcal{U}_j,\iota\mathcal{T}_j\right)\tilde{\varphi}(\mathbf{k};)J_0^2(x_{Lj})\right] \quad (1)$$

The first term on r.h.s corresponds to adiabatic response while the second term represents the non-adiabatic response. Also q_j, T_j are charge and temperature for species j, N equilibrium density. $\omega_j^* = \omega_{nj}\left[1+\frac{\eta_j}{2}\left(\frac{v_{||}^2}{v_{thj}^2}-3\right)+\frac{\eta_j v_\perp^2}{2\,v_{thj}^2}\right]$ with $\omega_{nj} = (T_j\nabla_n \ln N k_\theta)/(q_j B)$ is the *diamagnetic drift frequency*; $\eta_j = (d\ln T_j)/(d\ln N)$, $v_{||}$ and $v_\perp$ represent respectively parallel and perpendicular velocity, v_{thj} is the thermal velocity of species j. $J_0(x_{Lj})$ is the Bessel function of argument $x_{Lj} = k_\perp \rho_{Lj}$, taking into account full finite Larmor radius effect. We consider a local Maxwellian for each species of mass m_j as

$$f_{Mj}(\xi,\psi) = \frac{N(\psi)}{\left(\frac{2\pi T_j(\psi)}{m_j}\right)^{3/2}}\ \exp\left(-\frac{\xi}{T_j(\psi)/m_j}\right)$$

where $\xi = \frac{v^2}{2}$. In Eq.(1) the term $\mathcal{U}_j$ stands for the guiding center propagator of untrapped particles of type j=i (ion), e (electron), f (fast ions) while $\mathcal{T}_j$ represents the guiding center propagator for trapped particle j=i for the present case. The derivation of these propagators for both untrapped and trapped particles is given in detail in [10, 25, 30].
Introducing *quasi neutrality condition.*

$$\sum_j \tilde{q}_j\tilde{n}_j(\mathbf{r};\omega) \simeq 0; \quad (2)$$

$\tilde{q}_j$ being the charge of the species j one would finally end up with a generalized eigenvalue problem where ω and $\tilde{\varphi}$ respectively are eigenvalue and eigen-vector, This is then solved in Fourier space by Fourier decomposing the potential in Eq.(2) first and then taking Fourier transform, to eventually obtain a convolution matrix in Fourier space.

$$\sum_{\mathbf{k}'}\sum_{j=i}\mathcal{M}^j_{\mathbf{k},\mathbf{k}'}\ \tilde{\varphi}_{\mathbf{k}'} + \sum_{\mathbf{k}'}\sum_{j=tr-i}\mathcal{M}^j_{\mathbf{k},\mathbf{k}'}\ \tilde{\varphi}_{\mathbf{k}'} + \sum_{\mathbf{k}'}\sum_{j=e}\mathcal{M}^j_{\mathbf{k},\mathbf{k}'}\ \tilde{\varphi}_{\mathbf{k}'} + \sum_{\mathbf{k}'}\sum_{j=f}\mathcal{M}^j_{\mathbf{k},\mathbf{k}'}\ \tilde{\varphi}_{\mathbf{k}'} = 0$$

where $\mathbf{k} = (\kappa, m)$ and $\mathbf{k}' = (\kappa', m')$. For detail calculation the reader is referred to [26]

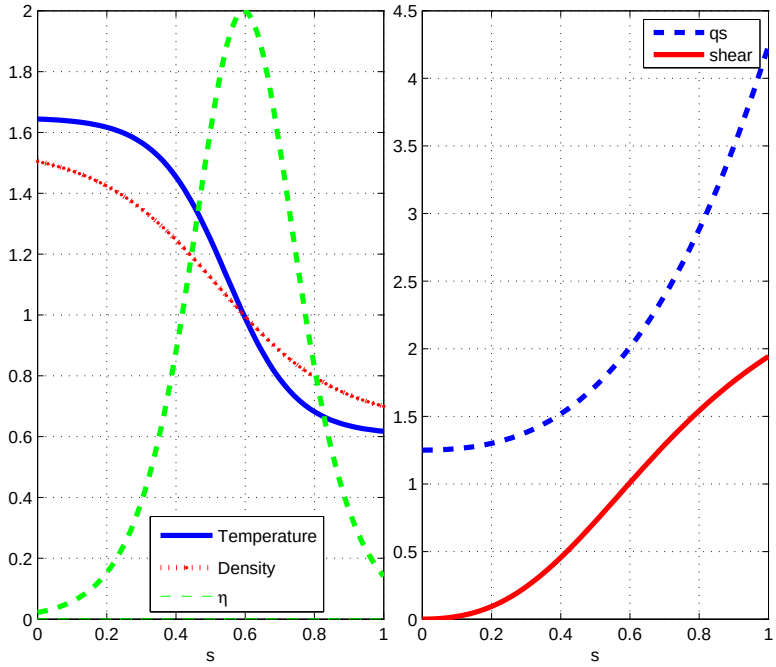

Figure 1. Equilibrium profiles for global ITG stability studies (parameters for Table-1). Normalized density, temperature, $\eta_{i,e,f}$ (left), Safety factor q and magnetic shear $\hat{s}$ profiles as functions of normalized radius $s = r/a$. Note that η peaks at $s = \rho/a = s_0 = 0.6$

3. Results & Discussion

Following are the profiles and parameters that are used in the analysis here. The corresponding equilibrium profiles are depicted in Fig.1.

Table 1. Parameters and Equilibrium Profiles

• B-field : $B_0 = 1.0$ Tesla	• N-profile and T-profile
• Temperature : $T_0 = T(s_0) = 7.5\ Kev$	$N(s)/N_0 = \exp\left(-\frac{a\ \delta s_n}{L_{n0}}\ \tanh\left(\frac{s-s_0}{\delta s_n}\right)\right)$
• Major Radius : $R = 2.0\ m$	$T_{i,e}(s)/T_0 = \exp\left(-\frac{a\ \delta s_T}{L_{T0}}\ \tanh\left(\frac{s-s_0}{\delta s_T}\right)\right)$
• Minor Radius : $a = 0.5\ m$	$\delta s_n = 0.35,\ \delta s_T = 0.2$ at $s = s_0$
• radius : $s = \rho/a\ \ 0.01 < s < 1.0,\ s_0 = 0.6$	• $q(s) = 1.25 + 0.67\ s^2 + 2.38\ s^3 - 0.06\ s^4$
• $L_{n0} = 0.4\ m,\ L_{T0} = 0.2\ m \rightarrow \eta_{i,e,f}(s_0) = 2.0$	such that $q(s = s_0) = 2.0$;
• $\tau(s) = T_e(s)/T_i(s) = 1,\ \rho^* \equiv \rho_{Li}(s = s_0)/a \simeq 0.0175$.	Shear $\hat{s}$ is positive and at $s = s_0,\ \hat{s} = 1$.

3.1. ITG mode with non-adiabatic electrons

Fig.2 depicts the growth rate and real frequency against the toroidal mode number n for the cases i. ITG with adiabatic electrons (open circle), then ITG with non-adiabatic passing electrons

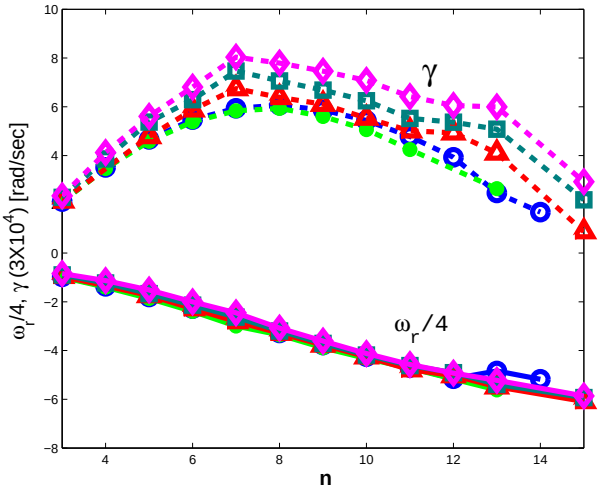

Figure 2. Growth rate γ and real frequency ω_r (i) for ITG with adiabatic electron model (open circle), (ii) ITG mode with non-adiabatic passing electrons for $\eta_e(s_0) = 2.0$(filled circles), $\eta_e(s_0) = 4.0$(triangle), $\eta_e(s_0) = 6.0$(square), $\eta_e(s_0) = 8.0$(diamond) with $\eta_i(s_0) = 2$ for all

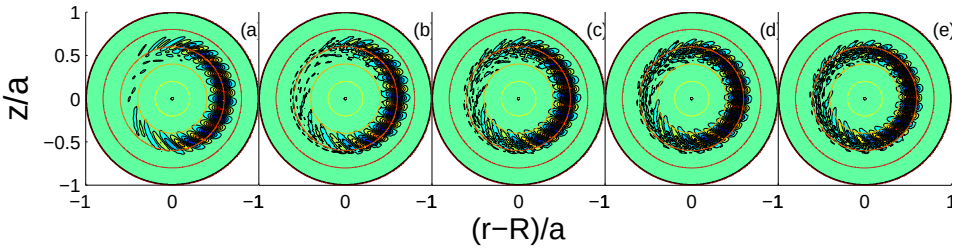

Figure 3. Mode structures (i) for ITG with adiabatic electron model (a), (ii) ITG mode with non-adiabatic passing electrons for $\eta_e(s_0) = 2$ (b), $\eta_e(s_0) = 4$ (c), $\eta_e(s_0) = 6$(d), $\eta_e(s_0) = 8$ (e) all for $\eta_i(s_0) = 2$

with η_e=2 (filled circle), $\eta_e = 4$ (triangle), $\eta_e = 6$ (square) and $\eta_e = 8$ (diamond). It is clear that

growth rate continuously increases as one goes from $\eta_e = 2$ to $\eta_e = 8$. The rise in the growth rate in comparison to the adiabatic case (open circle) is because of the reason that electrons with a non-adiabatic component in its response, can not follow a perturbation to short circuit the charge separation thereby enhancing the growth rate. Especially near the mode rational surfaces $k_\parallel = 0$, the phase velocity of perturbation $\frac{\omega_r}{k_\parallel} \to \infty$ and the electrons response is very sluggish near these mode rational surfaces. Since low n ITG can be quite global one can expect it to pass through several such mode rational surfaces and slow electrons near these surfaces leads to higher growth rate of the mode.

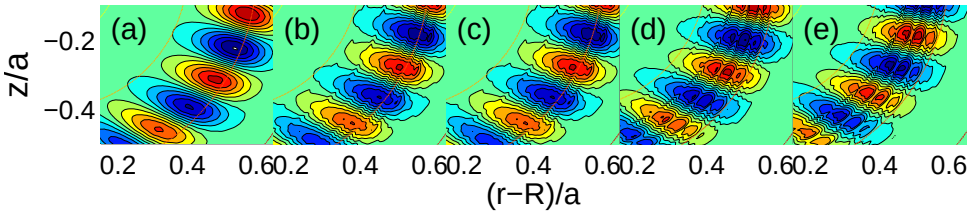

Figure 4. Close up view of mode structures displayed in Fig.3

The corresponding mode structure across the minor radius of the tokamak is shown in Fig.3 with their zoom in pictures displayed in Fig.4. One can see clearly the evolution of short scales in the mode structure while going from adiabatic case to non-adiabatic case with increasing η_e. The positions where the smooth structure break correspond to mode rational surface. This becomes clear if one looks at the Fig.5. where potential ϕ is plotted across the minor radius. At each radial position several poloidal modes are coupled. This coupling is brought about by the curvature of the system. The dots on the upper axis represent the position of mode rational surfaces characterized my $m = nq$. Spikes are clearly visible at points where $k_\parallel = 0$. The sudden rise in the potential is because of the inability of the electrons to move along the magnetic field and to wipe out the charge separation. The reduction in the scale-length takes place much faster than the growth rate. This is becomes apparent when one calculates the mixing-length estimation based transport presented in Fig.5 in gyro-Bohm unit. The transport coefficient goes on decreasing as one includes non-adiabaticity of electron and increases η_e despite the increase in the growth rate.

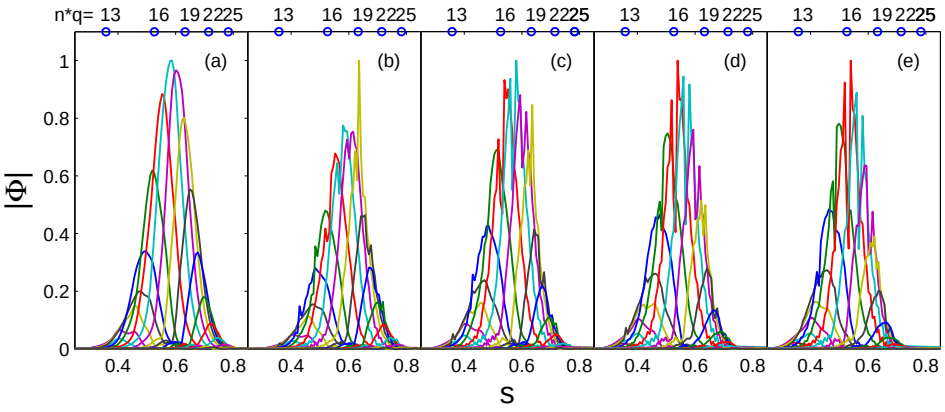

Figure 5. Poloidal Fourier components for the electrostatic modes shown in Fig.3. The coupling of several poloidal harmonics at each radial position is apparent. Top axis presents the position of mode rational surfaces. Non adiabatic electrons introduce sharp structure at these points.

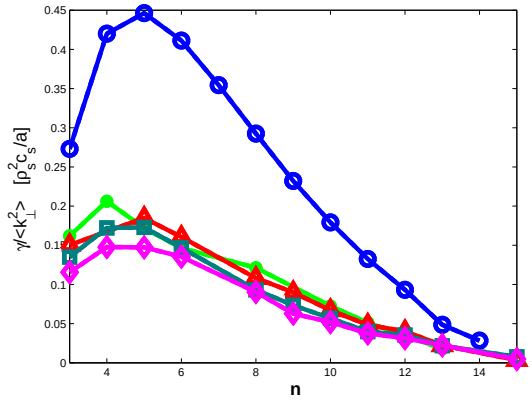

Figure 6. Mixing length based estimation of transport coefficient $D_{ML} = \frac{\gamma}{k_\perp^2 i}$ for (i) for ITG with adiabatic electron model (open circle),(ii) ITG mode with non-adiabatic passing electrons for $\eta_e(s_0) = 2.0$(filled circles), $\eta_e(s_0) = 4.0$(triangle), $\eta_e(s_0) = 6.0$(square), $\eta_e(s_0) = 8.0$(diamond) with $\eta_i = 2.0$ for all

3.2. ITG mode with fast ions

A perturbative treatment of impurity ions and consequent effect can be found in [27] where the impurities are observed to have stabilizing effect on the mode in the flat density limit. Hot

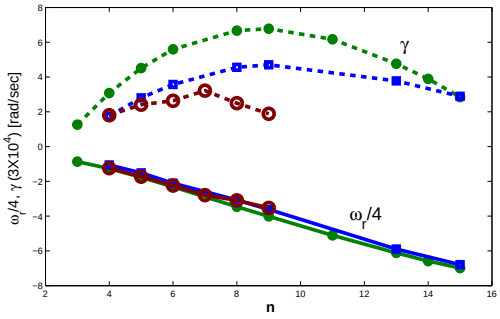

Figure 7. (a) Growth rates (b) frequencies for profiles in Fig.1. Growth rate γ and real frequency ω_r (i) for pure ITG without fast ion (filled circle), (ii)ITG mode with fast ions (square) and (iii) ITG mode with He ions in deuterium background (open circle). $\eta_e(s_0) = \eta_i(s_0) = \eta_f(s_0) = 2.0$, $\frac{T_f}{T_i} = 20$, $\frac{n_f}{n_e} = 0.1$

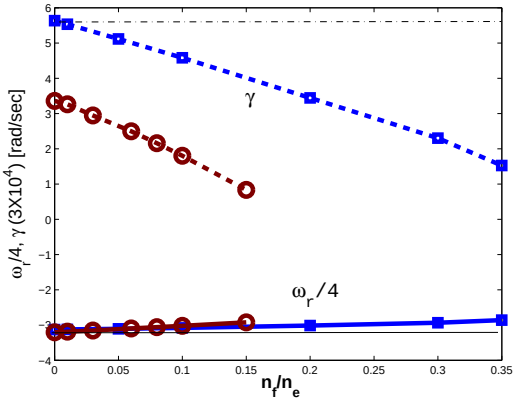

Figure 8. Growth rate γ and real frequency ω_r versus fast ion to electron density ratio $\frac{n_f}{n_e}$ for (i) ITG mode with fast ions (square) and (ii) ITG mode with He ions in deuterium background (open circle). Horizontal lines are for ITG mode without fast ions. $\eta_e(s_0) = \eta_i(s_0) = \eta_f(s_0) = 2.0$, $\frac{T_f}{T_i} = 20$

ions produced in the ion cyclotron resonance heating or neutral beam injection are found to have slight stabilizing influence on the toroidal ITG but produce significant reduction in ion heat flow [28]. Only recently these fast ion concentration is identified to be the key ingredient of the ion ITB formation suppressing ITG mode [29]. We here try to reveal the effect of hot ion concentration and temperature on the background ITG non-perturbatively. To investigate the effect of fast ions on the background ITG mode we first do a toroidal mode number scan of frequency and growth rate of the mode. Fig.7 presents the n scan of growth rate and real frequency for three cases i. ITG without fast ions ii. ITG with fast ions and iii. ITG with He ions produced in deuterium plasma. It is evident from the scan that the fast ions stabilizes the ITG mode. The stabilization can be attributed to the dilution of the background ions. He ions have more stabilizing effect than the single charged ions. The reason is that He ions bear double charge and dilution of ions is more. The dilution reduces the temperature gradient drive of the background ions. It is important to estimate the fraction of fast ion density required to

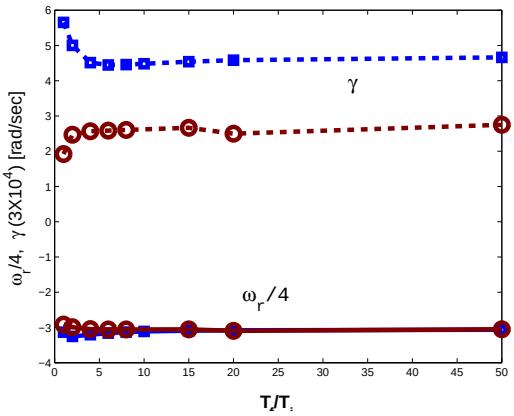

Figure 9. Growth rate γ and real frequency ω_r versus fast ion to electron temperature ratio $\frac{T_f}{T_i}$ for (i) ITG mode with fast ions (square) and (ii) ITG mode with He ions in deuterium background (open circle). $\eta_e(s_0) = \eta_i(s_0) = \eta_f(s_0) = 2.0$, $\frac{n_f}{n_e} = 0.1$

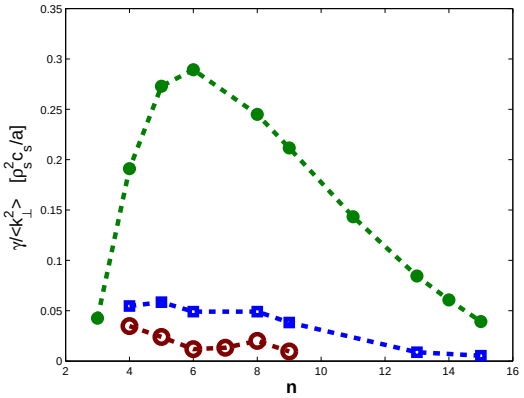

Figure 10. Mixing length based estimation of transport coefficient $D_{ML} = \frac{\gamma}{k_\perp^2 i}$ for (i) pure ITG without fast ion (filled circle), (ii)ITG mode with fast ions (square) and (iii) ITG mode with He ions in deuterium background (open circle). $\eta_e(s_0) = \eta_i(s_0) = \eta_f(s_0) = 2.0$, $\frac{T_f}{T_i} = 20$, $\frac{n_f}{n_e} = 0.1$

stabilize a mode. Fig.8 shows the growth rate and frequency when one increases the density fraction of fast ions. The mode gets almost stabilized at a value of $\frac{n_f}{n_e} = 0.35$. He ions stabilizes the mode faster in consistent with the observation in Fig.7. Almost complete stabilization happens to be at a value $\frac{n_f}{n_e} = 0.15$. The temperature dependence of fast ions is displayed in Fig.9. It is clear that the mode remains sensitive to fast ion to background ion temperature ratio $T_f/T_i \sim 7$. The possible reason is that ITG is a low frequency mode and the fraction of ions with higher temperature decouples completely at this value of temperature ratio. Mixing length estimation of transport is depicted in Fig.10 where the transport coefficient is plotted in gyro-Bohm unit against toroidal mode number n. The transport co-efficient decreases when one includes the single charged hot ions. With the presence of He ions the reduction in the mixing length transport is quite significant.

4. Conclusion

We in the present work have shown the effect of non-adiabatic passing electrons and fast ions on the ITG mode. The growth rate increases continuously with non-adiabatic electrons as one increase the η_e. These electrons break the ITG mode structure into small scales, thus reducing the scale length and the mixing length estimation of transport. Non perturbative fast ions on the other hand are found to have strong stabilizing effect on the ITG mode leading to reduction in transport.

References

[1] Horton W 1999 *Rev. Mod. Phys.* **71** 735
[2] Terry P 2000 *Rev. Mod. Phys.* **72** 1 109
[3] Liewer P C 1985 *Nucl. Fusion* **25** 543
[4] Rudakov L I and Sagdeev R J 1962 *Nuclear Fusion Suppl* **2** 481
[5] Dimits A M, Bateman G, Beer M A 2000*et al Phys. Plasmas* 969
[6] Coppi B and Pegoraro F 1977 *Nucl. fusion* **17** 969
[7] Parker S E, Lee W W and Santoro R A 1993 *Phys. Rev. Lett.* **71** 2042
[8] Dimits A M, Williams T J, Byers J A and Cohen B I 1996 *Phys. Rev. Lett.* **77** 71
[9] Sydora R D, Decyk V K and Dawson J M 1996 *Plasma Phys. Control. Fusion* **38** A281A294
[10] Brunner S, Fivaz M, Tran t M and Vaclavik J 1998 *Phys. Plasmas* **5** 11 3929
[11] Beer M A and Hammett G W 1996 *Phys. Plasmas* **3** 11 4018
[12] Fong B H and Hahm T S 1999, *Phys. Plasmas* **6** 188
[13] Lee W W, Lewandowski J L V, Hahm T S and Lin Z 2001 *Phys. Plasmas* **8** 4435
[14] Cheng C.Z., Nucl. Fusion 1982 **22** 773
[15] Redd A J, Kritz A H, Bateman G, Rewoldt G and Tang W M 1999 *Phys. Plasmas* 6
[16] Malinov P and Zonca F 2005 *J. Plasma Physics* **71** 3 pp.301-313
[17] Ross D and Dorland W 2002 *Phys. Plasmas* **9** 5031
[18] Candy J and Waltz R E 2002 *J. Comp. Physics* **186** 545
[19] Parker S E, Chen Y and Wan W 2004 *Phys. Plasmas* **11** 2594
[20] Falchetto G L, Vaclavik J and Villard L 2003 *Phys. Plasmas* **10** 5 1424
[21] Ganesh R, Angelino P, Vaclavik J and Villard L 2004 *Phys. Plasmas* **11** 3106
[22] Angelino P 2006 *Ph.D thesis* EPFL Switzerland Thesis no : 3559
[23] Ganesh R, Vaclavik J and Villard L, *Proc. of the Joint Varenna-Lausanne Int. Workshop on Theory of Fusion Plasmas* Villa Monastero - Varenna, Italy, August 2004, ed J W Connor, O Sauter and E Sindoni (Societa Italiana Di Fisica, Italy 2004)
[24] Angelino P, Bottino A, Falchetto G, Ganesh R, Vaclavik J and Villard L 2005 *Transp. Th. Stat. Phys.* **34** 333
[25] Ganesh R and Vaclavik J 2005 *Phys. Rev. Lett.* **94** 145002
[26] Brunner S 1997 *Ph.D thesis* EPFL Switzerland Thesis no : 1701
[27] Paccagnell R, Romanelli F, Briguglio S 1990 *Nuclear Fusion* **30** 3
[28] Liljestrom M 1990 *Nuclear Fusion* **30** 12
[29] Tardini *et al* 2007 *Nuclear Fusion* **47** 280-287
[30] Chowdhury J, Ganesh R, Angelino P, Vaclavik J, Villard L and Brunner S 2008 *Phys. Plasmas* **15** 072117-1